Lead optimization of the VU0486321 series of mGlu$_1$ PAMs. Part 2. SAR of alternative 3-methyl heterocycles and progress towards an *in vivo* tool

Pedro M. Garcia-Barrantes[a], Hyekyung P. Cho[a,b], Adam M. Metts[c], Anna L. Blobaum[a], Colleen M. Niswender[a,b], P. Jeffrey Conn[a,b], and Craig W. Lindsley[a,b,c,*]

[a]Vanderbilt Center for Neuroscience Drug Discovery, Vanderbilt University Medical Center, Nashville, TN 37232, USA

[b]Department of Pharmacology, Vanderbilt University School of Medicine, Nashville, TN 37232, USA

[c]Department of Chemistry, Vanderbilt University, Nashville, TN 37232, USA

Abstract

This letter describes the further lead optimization of the VU0486321 series of mGlu$_1$ positive allosteric modulators (PAMs), driven by recent genetic data linking loss of function *GRM1* to schizophrenia. Steep and caveat-laden SAR plagues the series, but ultimately potent mGlu$_1$ PAMs (EC$_{50}$s ~ 5 nM) have resulted with good DMPK properties (low intrinsic clearance, clean CYP profile, modest F$_u$) and CNS penetration (K$_p$s 0.25 to 0.97), along with up to >450-fold selectivity versus mGlu$_4$ and mGlu$_5$.

Graphical Abstract
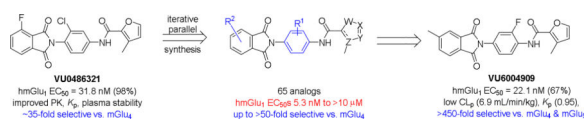
Keywords

mGlu$_1$; Metabotropic glutamate receptor; Positive allosteric modulator (PAM); Schizophrenia; Structure-Activity Relationship (SAR)

Driven by the recent reports of deleterious non-synonymous single nucleotide polymorphisms (nsSNPS) in the *GRM1* gene, which encodes the metabotropic glutamate receptor subtype 1 (mGlu$_1$), that correlated with a higher incidence of neuropsychiatric disease,[1,2,3] interest in mGlu$_1$ PAMs has increased.[3] *In vitro*, we have shown that mGlu$_1$

---

*To whom correspondence should be addressed: craig.lindsley@vanderbilt.edu.

PAMs can potentiate, and in some cases restore activity to wild-type levels in these mutants.[3] However, historical tools lacked the DMPK profiles to serve as robust *in vivo* tools.[3-6] En route to the ideal *in vivo* tool, our lab has published many advancements in the mGlu$_1$ PAM ligand field,[3,5,6] as well as demonstrating that the adverse effect of epilitiform discharges and seizure liability of Group I mGluR agonists, such as DHPG, is not mGlu$_1$ mediated,[5] and therefore widening the therapeutic window for mGlu$_1$ PAMs (**Figure 1**).

As previously discussed, our entry into the VU0486321 (**4**) series of mGlu$_1$ PAMs was via a 'double molecular switch' of an mGlu$_4$ PAM ligand.[3,7,8] While surveying a diverse array of 5-membered heterocyclic amides in the optimization effort, only a furyl amide was active, but substitution with a 3-methyl group, as in **4** and **5**, greatly enhanced mGlu$_1$ PAM potency.[5,6] However, we never went back and surveyed the impact of incorporation of a methyl moiety in the context of other 5-membered heterocycles, with more desirerable physiochemical and DMPK properties than a furyl ring (**Figure 2**). In this Letter, we will detail the steep and caveat-laden SAR en route to an *in vivo* tool compound within the VU0486321 (**4**) series of mGlu$_1$ PAMs.

In order to access analogs **6** and survey the SAR for the three regions highlighted in Figure 2, a general three step synthetic route was developed. As shown in **Scheme 1**, commercial, functionalized *p*-amino nitroarenes/heteroarenes **7** were condensed with various phthalic anhydrides to afford analogs **8**. The nitro group was reduced to the aniline **9** via hydrogenation conditons, and final analogs **6** were afforded by standard amide coupling conditions with a diverse array of 3-methyl substituted 5-membered heterocyclic acids.

For the initial library to survey alternative, 5-membered heterocyclic amides with a methyl group adjacent to the amide, we employed an unsubstituted phthalimide moiety and held the 3-chlorophenyl moiety constant. As shown in Table 1, this library afforded active mGlu$_1$ PAMs, and further highlights the impact of a methyl substituent (as *des*-methyl congeners were all inactive, EC$_{50}$s >10 μM).[6] However, not all analogs **10** were active, and even regioisomeric congeners displayed divergent SAR. In case of regioisomeric thiophenes, both **10d** and **10e** were equipotent, but weak mGlu$_1$ PAMs (EC$_{50}$s 1.5 to 1.8 μM); however, both oxadiazoles (**10f** and **10g**) and thiazoles (**10h** and **10i**) displayed divergent SAR, with the 5-methyl regioisomers **10g** and **10i** displaying potent PAM activity (EC$_{50}$s of 1.47 μM and 56 nM, respectively), while the 4-methyl regioisomers **10f** and **10h** were inactive (EC$_{50}$s >10 μM). An imidazole analog **10j** was also active (EC$_{50}$ = 374 nM), but strongly basic amines, such as the two enantiomeric, *N*-methyl prolines **10l** and **10m**, were inactive. These were very exciting findings overall, especially in the case of **10i**, a 56 nM mGlu$_1$ PAM, where a single methyl group increased potency almost 200-fold relative to the unsubstituted thiazole.[6] These data narrowed down the field to four methyl-substituted heterocycles (**10g**, **10i**, **10j** and **10k**) for further optimization in the context of functionalized phthalimides, and determine if SAR developed within the 3-furylamide series (**4** and **5**) would translate.

Next, we prepared a 4 × 7 matrix library to assess SAR of the four methyl-substituted heterocycles (**10g**, **10i**, **10j** and **10k**) in the context of seven differentially substituted (3-Me, 4-Me, 3-Cl, 4-Cl, 3-F, 4-F and 4-aza) phthalimide moieties (**Table 2**) to provide analogs **11**.

As mGlu$_4$ has been a pervasive anti-target, we also counter-screened the 28-membered library against mGlu$_4$, in singlicate, to understand any undesired off-target activity.

While the SAR was steep amongst the imidazole (**11o-u**) and pyrazole (**11v-bb**) congeners, the oxazole (**11a-g**) and thiazole (**11h-n**) uniformly provided potent mGlu$_1$ PAMs (EC$_{50}$s down to 22 nM) with a dynamic range of selectivity versus mGlu$_4$ (from 0.7- to > 52-fold). This lack of mGlu4 selectivity was not unexpected based on the central Cl-phenyl core from earlier SAR efforts. However, we were pleased to see that thiazoles and oxazoles could effectively replace the furyl moiety, even those analogs **11** could not advance as *in vivo* tools. Previously, we demonstrated that replacement of the Cl-phenyl core as in **4** and analogs **11**, with a fluorine atom in the 3-position (relative to the phthalimide moiety, as in **5**) maintained mGlu$_1$ PAM potency, while eliminating mGlu$_4$ activity (>793-fold selective).[6] Therefore, we synthesized analogs of **11a-n** to survey the impact of the regioisomer fluorine core (analogs **12**, **Table 3**) in a 10 μM single-point assay prior to running full CRCs. Surprisingly, none of these analogs were strong active mGlu$_1$ PAMs (<50% potentiation of EC$_{20}$ glutamate at 10 μM), highlighting once again the steep SAR challenges with allosteric ligands. Thus, it was clear that the more basic thiazole analogs could not be advanced due to the lack of selectivity versus mGlu$_4$, and that the SAR developed to abolish activity at mGlu$_4$ did not translate to the thiazoles.

The highly potent and selective mGlu$_1$ PAM **5**, was only prepared and evaluated in the context of an unsubstituted phthalimide moiety; therefore, it seemed prudent to further explore functionalized phthalimide analogs of **5**, and assess physiochemical properties and selectivity in hopes of developing a robust *in vivo* tool compound. Following the route outlined in Scheme 1, we synthesized five functionalized analogs **13a-e** (**Table 4**). Unlike the oxazole and thiazole congeners **12**, the furyl analogs **13** proved to be very potent mGlu$_1$ PAMs (EC$_{50}$s 5.3 to 25.7 nM), and both electron donating and electron withdrawing substituents were tolerated. As these new analogs **13** were equipotent or more potent than **5**, we assessed their disposition in a battery of *in vitro* and *in vivo* DMPK assays (**Table 5**).[9] All of the analogs displayed excellent CYP profiles (most IC$_{50}$s >30 μM against 3A4, 2C9, 2D6 and 1A2), low to moderate hepatic clearance in both rat (28.9 mL/min/kg to 52 mL/min/kg) and human (4.4 mL/min/kg to 11.9 mL/min/kg) microsomal incubations and exceptional free fraction in rat brain homogenate binding studies (F$_u$ 0.034 to 0.29), the latter suggesting high free drug levels in the CNS. Analogs **13** displayed high protein binding in both rat and human plasma (rapid equilibrium dialysis binding assay), and low recovery suggested modest instability in rat plasma *in vitro* (as noted previously due hydrolysis of the phthalimide).[5] However, the compounds were stable in human plasma, as well as rat brain homogenate, and importantly, *in vivo*. Analogs **13** were also CNS penetrant, with K$_p$s of 0.25 to 0.95 in rat PBL cassette studies. Therefore, all of these new analogs **13** were attractive and were potential *in vivo* mGlu$_1$ PAM tools compounds. In vivo rat PK after IV administration showed a wide range of clearance values (4.61 mL/min/kg to 65.5 mL/min/kg) and a disconnection from the *in vitro* predicted values (e.g., lack of IVIVC). Especially in the case of compound **13a** and **13b**, were clearance was, respectively, 8 and 4 times lower than the *in vitro* predicted value. It was also interesting to find a more rational trend in the *in vivo* clearance, where the electronic character and the position of the

substituents on the phthalimide moiety impacts the disposition of the compounds. From this study, compound **13b** emerged as the mGlu$_1$ PAM with the best pharmacokinetic profile to date (CL$_p$ = 6.94 mL/min/kg, t$_{1/2}$ = 4.75 h, V$_{ss}$ = 1.29 K/kg) and with high CNS penetration (K$_p$ = 0.95). Finally, we assessed selectivity versus mGlu$_4$ and mGlu$_5$, key anti-targets for this chemotype and found **13a**-**13e** were all uniformly inactive (>450 to >2,000-fold selective) against both mGlu$_4$ and mGlu$_5$ (EC$_{50}$s >>10 μM). Thus, potent, selective and CNS penetrant mGlu$_1$ PAMs were developed.

In conclusion, the continued optimization of the VU0486321 series of mGlu$_1$ PAMs has provided unique SAR, and highlighted the critical value of a single methyl group, a 'magic methyl' effect to engender PAM activity across a broad array of 5-member heterocycles. While we encountered instances of robust SAR, the classical steep SAR of allosteric modulators was noted, with key mGluR selectivity handles not translating to structurally similar chemotypes. However, revisiting the furyl amide congeners in the context of functionalized phthalimides, led to a sub-series of highly potent and CNS penetrant (Kps of 0.25 to 0.95) mGlu$_1$ PAMs, with favorable DMPK profiles (low CL$_p$, t$_{1/2}$s up to 4.9 hours and desirable volumes of distribution) and excellent selectivity profiles versus mGlu$_4$ and mGlu$_5$ (EC$_{50}$s >>10 μM, >450- to >2,000-fold selective). Of these, VU6004909 (**13b**) emerged as a near ideal rodent *in vivo* tool compound to probe selective mGlu$_1$ activation.

Acknowledgments

References

1. Frank RAW, McRae AF, Pocklington AJ, van de Lagemaat LN, Navarro P, Croning MDR, Komiyama NH, Bradley SJ, Challiss RAJ, Armstrong JD, Finn RD, Malloy MP, MacLean AW, Harris SE, Starr JM, Bhaskar SS, Howard EK, Hunt SE, Coffey AJ, Raganath V, Deloukas P, Rogers J, Muir WJ, Deary IJ, Blackwood DH, Visscher PM, Grant SGN. PLoS One. 2011; 6:e19011. [PubMed: 21559497]

2. Ayoub MA, Angelicheva D, Vile D, Chandler D, Morar B, Cavanaugh JA, Visscher PM, Jablensky A, Pfleger KDG, Kalaydijeva L. PLoS One. 2012; 7:e32849. [PubMed: 22448230]

3. Cho HP, Garcia-Barrantes PM, Brogan JT, Hopkins CR, Niswender CM, Rodriguez AL, Venable D, Morrison RD, Bubser M, Daniels JS, Jones CK, Conn PJ, Lindsley CW. ACS Chem. Bio. 2014; 9:2334–2346. [PubMed: 25137254]

4. Vieira E, Huwyler J, Jolidon S, Knoflach F, Mutel V, Wichmann J. Bioorg. Med. Chem. Lett. 2009; 19:1666–1669. [PubMed: 19233648]

5. Garcia-Barrantes PM, Cho HP, Niswender CM, Byers FW, Locuson CW, Blobaum AL, Xiang Z, Rook JM, Conn PJ, Lindsley CW. J. Med. Chem. 2015; 58:7959–7571. [PubMed: 26426481]

6. Garcia-Barrantes PM, Cho HP, Niswender CM, Blobaum AL, Conn PJ, Lindsley CW. Bioorg. Med. Chem. Lett. 2015; 25:5107–5110. [PubMed: 26476971]

7. Jones CK, Engers DW, Thompson AD, Field JR, Blobaum AL, Lindsley SR, Zhou Y, Gogliotti RD, Jadhav S, Zamorano R, Daniels JS, Morrison R, Weaver CD, Conn PJ, Lindsley CW, Niswender CM, Hopkins CR. J. Med. Chem. 2011; 54:7639–7647. [PubMed: 21966889]

8. Wood MR, Hopkins CR, Brogan JT, Conn PJ, Lindsley CW. Biochemistry. 2011; 50:2403–2410. [PubMed: 21341760]

9. Gentry PR, Kokubo M, Bridges TM, Byun N, Cho HP, Smith E, Hodder PS, Niswender CM, Daniels JS, Conn PJ, Lindsley CW, Wood MR. J. Med. Chem. 2014; 57:7804–7810. [PubMed: 25147929]
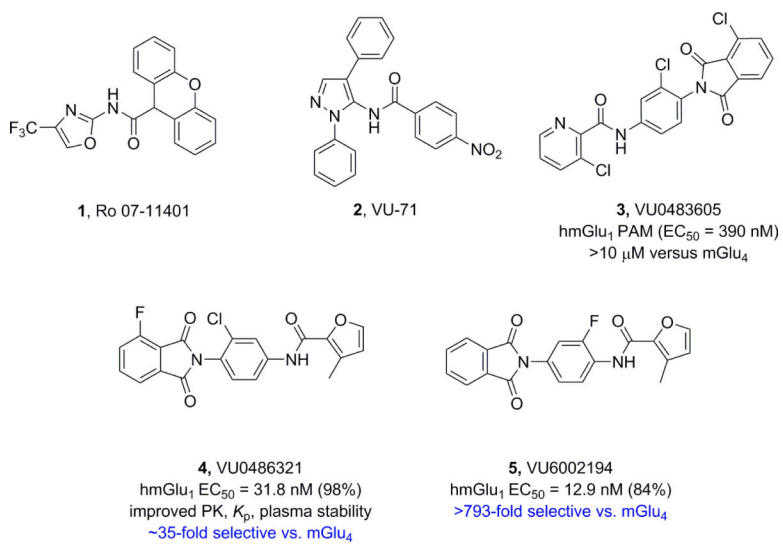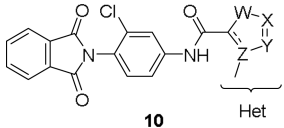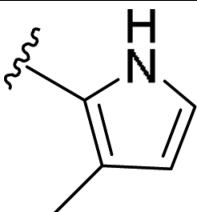
Figure 1.
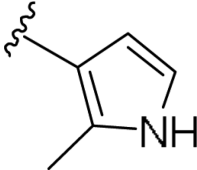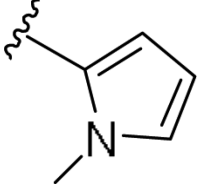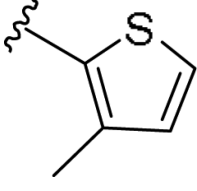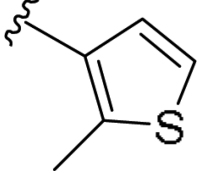Structures of representative mGlu$_1$ PAMs **1-5**.
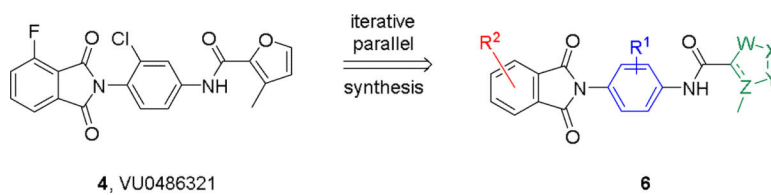
Figure 2.
Chemical optimization plan to access multi-dimensional SAR around analogs **6**.
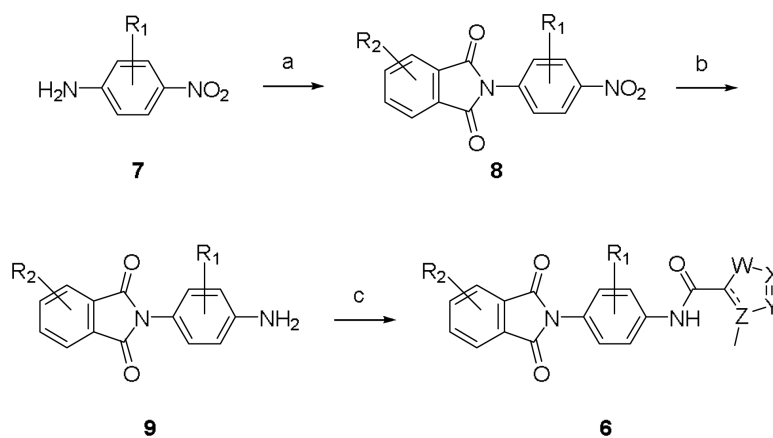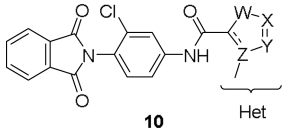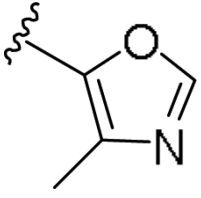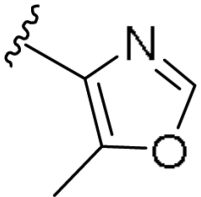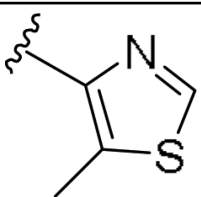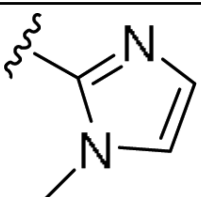
Scheme 1.
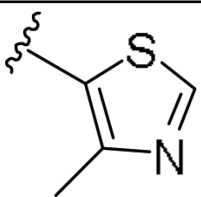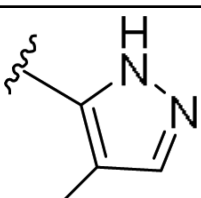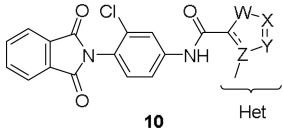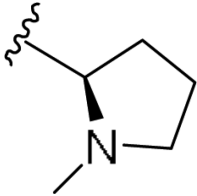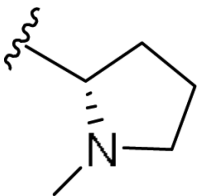Reagents and conditions: (a) phthalic anhydrides, AcOH, reflux, 53-94%; (b) H_2, Pd/C, EtOH, rt, 94-99-%; (c) methyl substituted 5-membered heterocyclic acids, HATU, DCM, r.t., 39-98%.

Table 1

Structures and activities for analogs 10.

Cpd	Het	hmGlu$_1$ EC$_{50}$ (μM)^a [% Glu Max ±SEM]	mGlu$_1$ pEC$_{50}$ (±SEM)
10a		3.42 [95±8]	5.46±0.13
10b		>10 [-]	>5
10c		5.26 [95±4]	5.28±0.10
10d		1.89 [105±11]	5.72±0.27
10e		1.51 [105±8]	5.82±0.17

Cpd	Het	hmGlu$_1$ EC$_{50}$ (μM)^a [% Glu Max ±SEM]	mGlu$_1$ pEC$_{50}$ (±SEM)
10f		>10 [-]	>5
10g		1.47 [100±17]	5.83±0.02
10h		>10 [-]	>5
10i		0.056 [96±7]	7.23±0.13
10j		0.374 [59±1]	6.45±0.13
10k		1.24 [107±11]	5.91±0.21
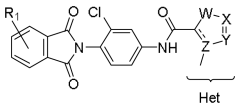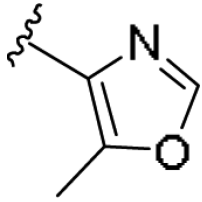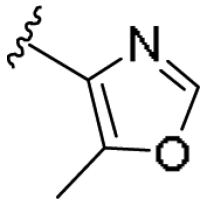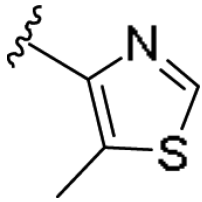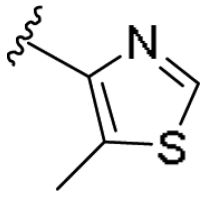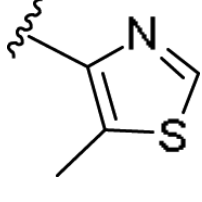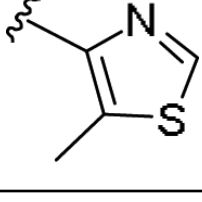
Cpd	Het	hmGlu$_1$ EC$_{50}$ (μM)^a [% Glu Max ±SEM]	mGlu$_1$ pEC$_{50}$ (±SEM)
10l		>10 [-]	>5
10m		>10 [-]	>5
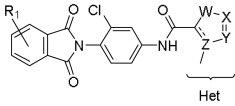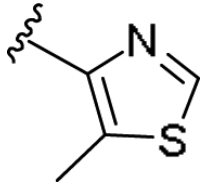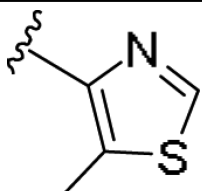
^{a}Calcium mobilization mGlu$_1$ assays, values are average of three (n=3) independent experiments performed in triplicate.
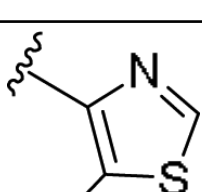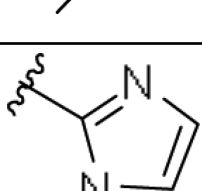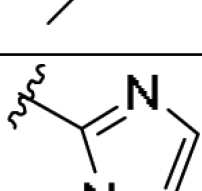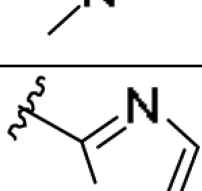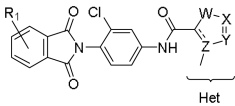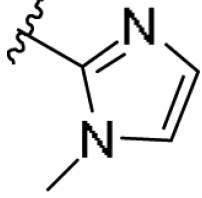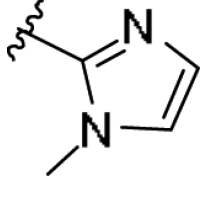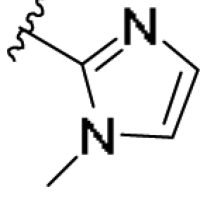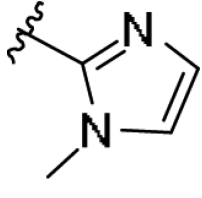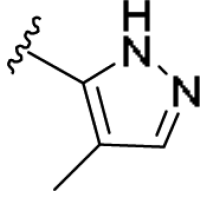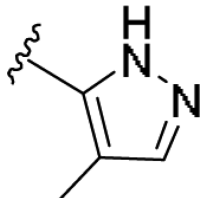
Table 2
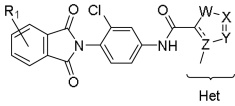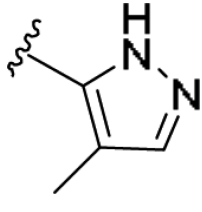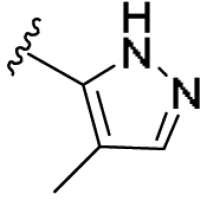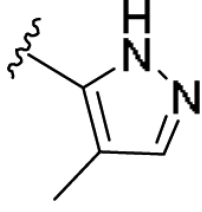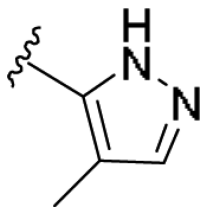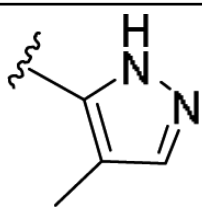
Structures and activities for analogs 11.

Cpd	R^1	Het	hmGlu$_1$ EC$_{50}$ (μM)^a [% Glu Max ±SEM]	mGlu$_1$ pEC$_{50}$ (±SEM)	hmGlu$_4$ EC$_{50}$ (μM) [% Glu Max^b]	Fold versus mGlu$_4$
11a	3-Me		0.041 [98±2]	7.38±0.11	0.198 [75]	4.8
11b	4-Me		0.469 [91±5]	6.32±0.13	0.519 [39]	0.9
11c	3-Cl		0.054 [104±4]	7.26±0.13	0.405 [67]	7.4
11d	4-Cl		1.29 [112±15]	5.88±0.26	0.983 [24]	0.7
11e	3-F		0.141 [93±3]	6.85±0.09	0.642 [36]	4.6

Cpd	R^1	Het	hmGlu$_1$ EC$_{50}$ (μM)^a [% Glu Max $\pm$SEM]	mGlu$_1$ pEC$_{50}$ ($\pm$SEM)	hmGlu$_4$ EC$_{50}$ (μM) [% Glu Max^b]	Fold versus mGlu$_4$
11f	4-F		0.241 [98±7]	5.77±0.18	>10 [-]	1.7
11g	4-Aza		1.70 [91±8]	5.77±0.18	2.53 [45]	>5.9
11h	3-Me		0.022 [86±2]	7.66±0.12	1.12 [161]	51.1
11i	4-Me		0.232 [104±5]	6.64±0.14	1.41 [75]	6.1
11j	3-Cl		0.051 [91±3]	7.30±0.15	1.98 [169]	39.1
11k	4-Cl		1.37 [121±12]	5.86±0.28	>10 [59]	>7.3

Cpd	R^1	Het	hmGlu$_1$ EC$_{50}$ (µM)^a [% Glu Max ±SEM]	mGlu$_1$ pEC$_{50}$ (±SEM)	hmGlu$_4$ EC$_{50}$ (µM) [% Glu Max^b]	Fold versus mGlu$_4$
11l	3-F		0.063 [98±4]	7.20±0.14	0.306 [52]	4.9
11m	4-F		0.187 [111±6]	6.73±0.16	0.474 [52]	2.5
11n	4-Aza		0.191 [98±4]	6.72±0.11	>10 [-]	>52
11o	3-Me		0.254 [108±8]	6.60±0.20	0.602 [124]	2.4
11p	4-Me		±10 [30±1]	>5	0.506 [32]	-
11q	3-Cl		0.265 [103±5]	6.58±0.13	1.573 [145]	5.9

Cpd	R^1	Het	hmGlu$_1$ EC$_{50}$ (μM)^a [% Glu Max ±SEM]	mGlu$_1$ pEC$_{50}$ (±SEM)	hmGlu$_4$ EC$_{50}$ (μM) [% Glu Max^b]	Fold versus mGlu$_4$
11r	4-Cl		±10 [30±1]	>5	>10 [30]	-
11s	3-F		0.673 [87±4]	6.17±0.12	1.07 [63]	1.5
11t	4-F		±10 [43±9]	>5	1.09 [42]	-
11u	4-Aza		±10 [44±8]	>5	>10 [-]	-
11v	3-Me		0.557 [106±7]	6.25±0.16	2.75 [133]	4.9
11w	4-Me		4.94 [110±15]	5.36±0.22	>10 [-]	>2
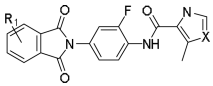
Cpd	R¹	Het	hmGlu₁ EC₅₀ (µM)ᵃ [% Glu Max ±SEM]	mGlu₁ pEC₅₀ (±SEM)	hmGlu₄ EC₅₀ (µM) [% Glu Maxᵇ]	Fold versus mGlu₄
11x	3-Cl		0.855 [113±5]	6.07±0.09	3.38 [117]	3.9
11y	4-Cl		±10 [94±2]	>5	>10 [-]	-
11z	3-F		0.632 [106±5]	6.20±0.17	6.20 [59]	9.8
11aa	4-F		0.599 [83±6]	7.65±0.13	>10 [-]	>16
11bb	4-Aza		>10 [37±9]	>5	>10 [27]	-

ᵃCalcium mobilization mGlu₁ assays, values are average of three (n=3) independent experiments performed in triplicate.

ᵇGlu Max is expressed as % of PHCCC response.

Table 3
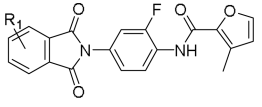
Structures and activities for analogs 12.

Cpd	R^1	X	% Glu Max (10 μM)^a	Cpd	R^1	X	% Glu Max (10 μM)^a
12a	H	O	18	12i	H	S	45
12b	3-Me	O	14	12j	3-Me	S	36
12c	4-Me	O	20	12k	4-Me	S	17
12d	3-Cl	O	25	12l	3-Cl	S	40
12e	4-Cl	O	27	12m	4-Cl	S	22
12f	3-F	O	16	12n	3-F	S	45
12g	4-F	O	36	12o	4-F	S	43
12h	4-Aza	O	9	12p	4-Aza	S	42

^{a}Calcium mobilization mGlu$_1$ assays, single point at 10 μM.

Table 4

Structures and activities for analogs 13.

Cpd	R^1	hmGlu$_1$ EC$_{50}$ (nM)^a [% Glu Max ±SEM]	mGlu$_1$ pEC$_{50}$ (±SEM)
13a	3-Me	11.4 [81±2]	7.94±0.05
13b	4-Me	25.7 [70±2]	7.59±0.04
13c	3-Cl	5.3 [60±2]	8.27±0.02
13d	3-F	19.3 [81±2]	7.71±0.06
13e	4-F	22.0 [67±2]	7.65±0.07

^{a}Calcium mobilization mGlu$_1$ assays, values are average of three (n=3) independent experiments performed in triplicate.

Table 5

DMPK Characterization of mGlu$_1$ PAMs 13a-e.

Parameter	13a	13b	13c	13d	13e
Hum CL$_{hep}$ (ml/min/kg)	4.40	6.64	11.9	6.72	4.48
Rat CL$_{hep}$ (ml/min/kg)	35.0	28.9	46.7	52.0	35.8
Hum F$_u$ plasma	0.002	0.009	<0.001	0.03	0.027
Rat F$_u$ plasma[a]	0.009	0.038	0.001	0.011	0.011
Rat F$_u$ brain	0.193	0.298	0.272	0.17	0.034
CYP$_{450}$ IC$_{50}$ (µM)					
1A2 2C9	10 >30	>30 >30	6.3 >30	>30 >30	>30 >30
2D6 3A4	>30 >30	>30 >30	>30 >30	>30 >30	>30 >30
Rat iv PK (0.25 mg/kg)					
$t_{1/2}$ (min)	296	285	51.5	38.9	76.6
MRT (min)	330	186	45.4	30.7	80.4
Cl$_p$ (mL min^{-1} kg^{-1})	4.61	6.94	65.5	62.6	16.7
V$_{ss}$ (L/kg)	1.52	1.29	2.97	1.92	1.34
Rat iv PBL (0.25 mg/kg)					
C$_n$ plasma (ng/mL)	699	191	217	0.97	151
C$_n$ Brain (ng/g)	177	182	120	147	97.2
K$_p$ (at 0.25 h)	0.25	0.95	0.55	0.95	0.64

[a] Indicates moderate compound instability in rat plasma *in vitro.*